Environmental Earth Sciences (2018) 77:93
https://doi.org/10.1007/s12665-018-7271-3

ORIGINAL ARTICLE

Multi-satellite-based water budget components in South Korea

Jongjin Baik[1] · **Minha Choi**[2]

Received: 29 May 2017 / Accepted: 20 January 2018 / Published online: 2 February 2018

Abstract
Interpreting and predicting variations of the water cycle are a significant concern given the emerging threat of climate change. Generically, hydrological components of the water cycle are routinely observed with ground-based measurements, yet it is difficult to measure their spatiotemporal variability. Remote sensing approach is recognized as one of the most promising tools to obtain continuous data over large areas, thereby offering the unique possibility to assess the complicated and non-local features of hydrological phenomena. To estimate water budget components using remote sensing, this research considers precipitation (P), evapotranspiration (ET), and the change in water storage (ΔS) calculated from satellites (i.e., Communication, Ocean and Meteorological Satellite; COMS, and Gravity Recovery and Climate Experiment; GRACE) and the Global Land Data Assimilation System (GLDAS) model-based datasets in South Korea from April to December 2011. The P estimates from the COMS rainfall intensity (COMS RI), COMS CM (which employs conditional merging [CM] to improve the accuracy of COMS RI), and GLDAS were compared with the measured P values from the two flux towers on a monthly scale. These results showed that COMS CM and GLDAS are in reasonable agreement, and additionally, their correlation, bias, and root-mean-square errors are favorable compared to the original COMS RI. The ET estimation of GLDAS and COMS applied from the revised RS-PM method were compared which indicated reasonable agreement with the two flux tower measurements. The derived runoff from COMS RI, COMS CM, and GLDAS was evaluated with that of the flux towers. The statistical results indicated that COMS CM and GLDAS were slightly better than that of COMS RI. The spatial distribution of P from COMS CM and GLDAS indicated similar pattern with that of ground-based measurement with the exception of COMS RI. ET from COMS and GLDAS showed slightly analogous pattern. The spatial distribution of runoff from both COMS and GLDAS showed evidence of a seasonality, which mainly resulted from the seasonally varying effects of ET and P. This research shows that it is possible to conduct the analysis of COMS products for efficient water resource planning, monitoring, and water budget modeling.

Keywords COMS · Water budget · GRACE · GLDAS · South Korea

Introduction

Under the warming that frequently accompanies global climate change, there is a potential increase in the rate of major natural disasters, and altered hydro-meteorological variables may significantly affect both human life and socioeconomic conditions (Mitsch and Gosselink 2000; Thomas et al. 2014). Regrettably, the issue of worldwide climate change on water resources is rather hard to define precisely (Oki and Kanae 2006). The hydrological cycle is expected to become more extreme, and thus, the quantification of hydrology and related energy cycles are crucial for understanding the feedbacks and relationships between essential water and energy components (Sahoo et al. 2011).

The traditional way of detecting key components of the hydrological cycle is through the use of traditional ground-based measurements. However, in many cases, ground-based observations are not suitable to be used in quantification of data over a large area due to the lack of consistency, transparency, quality of data, scarcity of dense in situ

✉ Minha Choi
mhchoi@skku.edu

Jongjin Baik
jjbaek@skku.edu

[1] Center for Built Environment, Sungkyunkwan University, Suwon 440-746, Republic of Korea

[2] Department of Water Resources, Graduate School of Water Resources, Sungkyunkwan University, 2066, Seobu-ro, Jangan-gu, Suwon, Gyeonggi-do 440-746, Republic of Korea

measurements, and high cost of establishing the infrastructure and management for such observations (Sheffield et al. 2009; Thiemig et al. 2012; Oliveira et al. 2014). Therefore, for many applications, it is a challenge to draw conclusions from research and analysis restricted only to ground-based observations. Satellite remote sensing has the potential to provide unprecedented spatiotemporal resolutions and to overcome the limitations of ground measurements, especially with regard to giving continuous estimates of the water cycle over regional and even global scales (Sheffield et al. 2009). As a result of the development of science and technology, novel approaches for the retrieval of hydrological components have been developed that are estimated from remote sensed datasets (Munier et al. 2014). In addition, the various observational products from satellites can be quantified, either specifically or generically, across various scales of time and space (Sahoo et al. 2011; Sheffield et al. 2009). Furthermore, the increasing number of satellite products provides a chance to understand phenomenon of water balance and budget at regional and at global scale (Wang et al. 2014). Commonly, the water budget is composed of the four major components: precipitation (P), evapotranspiration (ET), runoff (R), and the change in water storage (ΔS) at the Earth's surface. Examples of precipitation products include the Tropical Rainfall Measuring Mission (TRMM), the Global Precipitation Measurement (GPM), the Global Satellite Mapping of Precipitation Microwave-IR Combined Product (GSMaP_MVK), the Climate Prediction Center (CPC) MORPHing (CMORPH), and Precipitation Estimation from Remotely Sensed Information using Artificial Neural Networks (PERSIANN). The aforementioned precipitation products use data from recent and ongoing satellite missions, while using a variety of infrared and microwave sensor-based rainfall retrieval techniques, and can be used to cover the various regions of the world (Sheffield et al. 2009; Baik et al. 2016). Global evapotranspiration, which is estimated from energy balance and empirical models using satellite-based net radiation, vegetation characteristics, and meteorology parameters, can be obtained from the MODIS Global Evapotranspiration Project (MOD16) and Global Land Evaporation: the Amsterdam Model (GLEAM) (Miralles et al. 2011). Despite the importance of the change in water storage, it is not easy to measure at large scales because of the lack of adequate monitoring. In addition, there is a great deal of local spatial variability, and there are non-uniform local observations of variables such as ground water and soil moisture (Li et al. 2016). Therefore, to detect and quantify the water storage variation and hydrology fluxes for validation of water balance models, the Gravity Recovery And Climate Experiment (GRACE) has been applied at a global scale (Li et al. 2016). The use of hydrological components having high spatiotemporal resolution makes it possible to understand trends of the water budget and cycle (Oliveira et al. 2014). The water budget model, using hydrological components of various satellite products on local and global scales, has been studied in previous works (Sahoo et al. 2011; Sheffield et al. 2009; Oliveira et al. 2014; Munier et al. 2014; Wang et al. 2014). However, most previous studies focused on the Northern Hemisphere and Australia at the basin scale (Wang et al. 2014; Oliveira et al. 2014). These studies utilized multiple satellite-based hydrological products to improve and examine the water balance. However, it is difficult to definitively characterize the water budget due to the uncertainties of products and the spatiotemporal mismatches between satellite products (Wang et al. 2014). These studies also demonstrated that the largest uncertainty in the components of the overall water balance results from the large error of remotely sensed precipitation (Sheffield et al. 2009; Oliveira et al. 2014).

The primary objective of this study is to investigate hydrological components estimated from the Communication, Ocean and Meteorological Satellite (COMS), which is a geostationary satellite, and assess the water budget over South Korea, which has a complex and mountainous terrain. Further, we also improved the quantification of precipitation using a merging technique (i.e., conditional merging; CM) for reducing the uncertainty of precipitation of the COMS product. In addition, we use the GRACE dataset to estimate the change in water storage. Finally, we compared the results of the water budget equation, which are estimated from the COMS and Global Land Data Assimilation System (GLDAS) products, to the measurements at the two flux tower sites, and analyzed quantitatively and qualitatively to assess the spatial patterns of the GLDAS and COMS dataset from April to December 2011.

Data and methodology

Study area

South Korea (32.51N–40.00N, 124.49E–130.00E) is located in Far East Asia and has a relatively heterogeneous land cover, with mountainous terrain covering approximately 70% of the area. South Korea's latitude results in four distinctive seasons of spring, summer, autumn, and winter (Fig. 1). Both the spring and fall seasons in South Korea have relatively dry weather because of a migratory anticyclone. The mean annual precipitation and temperature in the study area ranges from 859.1 to 1403.8 mm (~ 60–70% of the annual average precipitation falls during the monsoon season) and from 10 to 15 °C with January and August as the coldest (− 6 to 3 °C) and the hottest (23–26 °C) months, respectively (Im et al. 2016). This study area is categorized as a region that suffers from

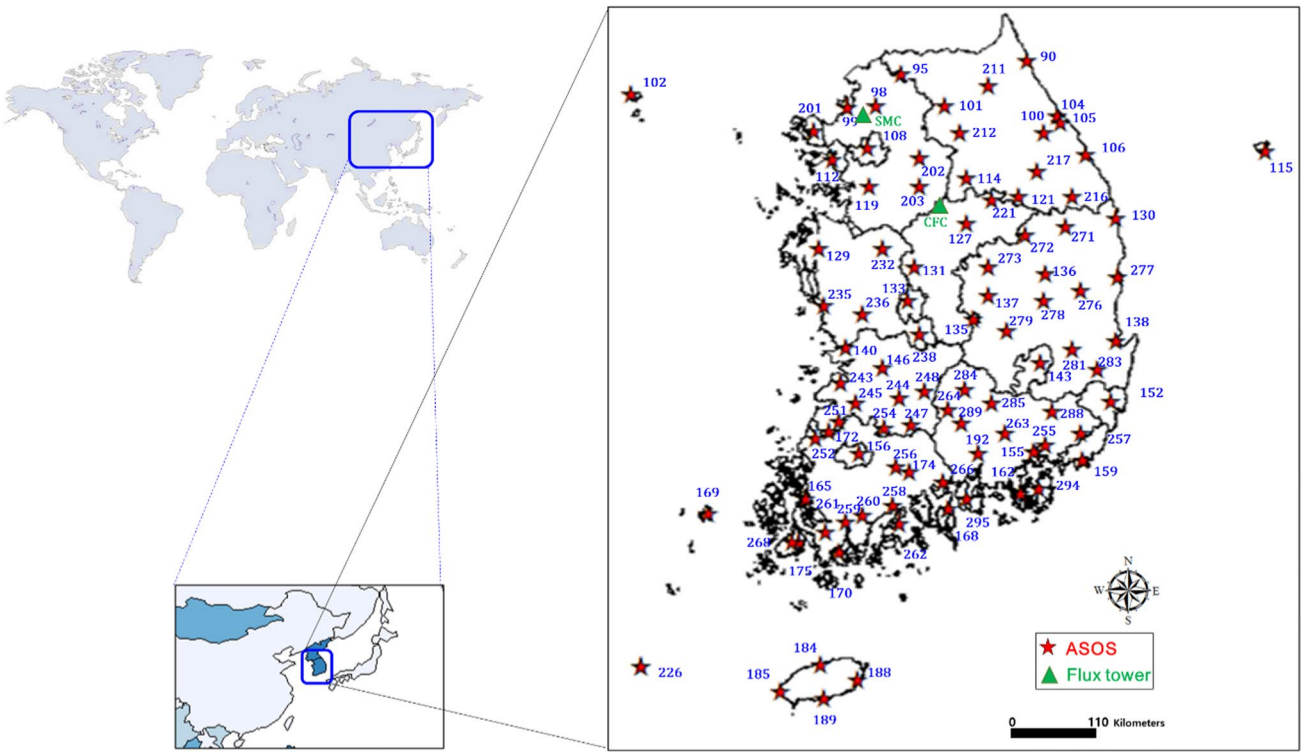

Fig. 1 Geographical location of the ASOS and flux tower sites

water shortage with heterogeneous topography and vegetation conditions (Kang et al. 2003; Park and Lee 2007; Nam et al. 2015).

The data quality of the Automatic Synoptic Observation System (ASOS) sites was maintained using the Korean Meteorological Administration (KMA). Further, we obtained ground-based precipitation data taken at 1-h intervals, from the Water Management Information System (WAMIS). As mentioned above, in order to improve the reliability of satellite-based precipitation data, this study utilized a conditional merging method, which leverages the benefits of each dataset (i.e., 93 ASOS sites and satellite-based datasets). Specific site characteristics are detailed in Fig. 1 and Table 1.

To evaluate the monthly evapotranspiration estimates of COMS and GLDAS, ground-based evapotranspiration was obtained from flux tower sites based on eddy covariance systems. The Sulma (SMC) and Cheongmi (CFC) flux towers, managed by the Hydrological Survey Center (HSC), provide ET data at half hour intervals and are used to obtain meteorological and energy flux datasets from April 01 to December 31, 2011. These sites have two different land cover types: mixed forest cover for the SMC site and rice farmland for the CFC site (Park et al. 2017). To measure the net radiation, two CNR-2 (Kipp & Zonen Inc., Delft, Netherlands) flux towers have been installed at 9.7 m and 19.2 m above the ground surface at the CFC and SMC, respectively. Moreover, at the flux tower sites, 3D sonic anemometers

Table 1 Summary of the different dataset (i.e., observation and satellite– and model-based datasets) containing data sources (i.e., precipitation (P), evapotranspiration (ET), change of water storage (ΔS)

Name	Dataset	Source	Resolution		Reference
			Spatial	Temporal	
COMS	ET, P	Satellite	0.01°, 0.04°	15 min	Baik and Choi (2015a, b, c, 2016)
GLDAS	ET, P	Reanalysis	0.25°	3 h, Monthly	https://ldas.gsfc.nasa.gov/gldas/
GRACE	ΔS	Satellite	0.5°	Monthly	http://grace.jpl.nasa.gov/
ASOS	P	Gauges	–	30 min	http://www.kam.go.kr/ http://www.wamis.go.kr/
Flux tower	ET, P	Gauges	–	30 min	http://hsc.re.kr/

The reference for the used dataset are as follows: COMS RI (Baik and Choi 2015a, b, c, 2016) COMS ET (Baik and Choi 2015a, b, c, 2016)

and open-path CO_2/H_2O analyzers, have been installed for observing the sensible heat flux and latent heat flux (2.1, 3.5, and 10.2 m in CFC; 2.0, 15.0, and 19.2 m in SMC), using the eddy covariance. A data logger (CR3000, CR800, and CR1000, Campbell Scientific Inc., USA) is used for recording the data.

COMS

COMS, Korea's first geostationary multi-purpose satellite, was launched on June 27, 2010 (Park et al. 2011). It was equipped with two types of sensors, the Meteorological Imager (MI) managed by the National Meteorological Satellite Center (http://nmsc.kma.go.kr/) and the Geostationary Ocean Color Imager (GOCI) managed by the Korea Ocean Satellite Center (http://kosc.kordi.re.kr/) (Ryu et al. 2012; Baik and Choi 2015b). In this study, we use the MI sensor product, which provides 16 meteorological factors (i.e., cloud analysis, cloud-top temperature/pressure, atmospheric motion vectors, cloud detection, etc.). The MI sensor with five bands (visible, shortwave, infrared, water vapor, infrared 1, and infrared 2) records the data at 15-min intervals and at 1- and 4-km spatial resolutions, covering most of Asia and Australia.

To estimate evapotranspiration from COMS, this study used a revised RS-PM model presented by Mu et al. (2007). Fundamentally, a revised RS-PM model, based on the Penman–Monteith equation, considers both vegetation transpiration and soil evaporation to calculate evapotranspiration (Baik and Choi 2015a; Mu et al. 2007; Sahoo et al. 2011). The detailed description of the COMS ET calculation implemented in this study can be found in Baik and Choi (2015b).

Among the COMS products, the COMS Rainfall Intensity (RI), provided by the NMSC, is based on the infrared rainfall retrieval method (An 2007; Baik and Choi 2015c). The COMS RI dataset has a temporal resolution of 15-min and a spatial resolution of 4 km. A previous study was dedicated to the assessment of the COMS RI (Baik and Choi 2015c). Baik and Choi (2015c) validated the satellite-based observations (COMS RI and TRMM 3B42 V7) with reference to ground-based measurements over the center of South Korea at different time scales. Their results indicated that COMS RI potentially succeeded in detecting the spatial variability of precipitation. Moreover, they also reported the need for improving the accuracy of quantitative precipitation estimates from COMS RI due to the limitation of the infrared rainfall retrieval method. In order to overcome this problem, previous researchers have developed various merging techniques that combine precipitation from point measurements and remote sensing techniques and hence have taken advantage of the complementary merits of each dataset (Woldemeskel et al. 2013; Sinclair and Pegram 2005). Baik et al. (2016) utilized three merging techniques (CM, Geographic Difference Analysis, and Geographic Ratio Analysis) for improving the satellite-based rainfall product. The results indicated that three different merging techniques showed the capability to improve the accuracy of COMS RI. In particular, the CM technique showed better results than the other merging techniques. The detailed information for improving precipitation estimates using the CM method and the COMS data, as well as the description of COMS, are given in Baik et al. (2016).

GLDAS

The GLDAS dataset is obtained by the combination of satellite and ground-based measurements through the four models: the Common Land Model (CLM), the Mosaic Land Surface Model (LSM), the Noah LSM, and the Variable Infiltration Capacity (VIC) model, which provides 3-hourly and monthly datasets with 0.25 and 1.0-degree spatial resolution datasets (Rodell et al. 2004; Baik and Choi 2015b) (Table 1). The detailed description of GLDAS is available at NASA's Hydrology Data and Information Services Center (http://disc.sci.gsfc.nasa.gov/hydrology). In this study, we used the GLDAS 0.25° products of version 1 (GLDAS_NOAH025_M), which were obtained from the NASA Land Information System and Goddard Earth Sciences Data and Information Services Center (Marshall et al. 2013).

GRACE

The GRACE satellite was launched for observing tiny changes in the Earth's gravitational field by measuring the distance between two orbiting satellites, launched in 2002 (Lee et al. 2014; Ramillien et al. 2008; Schmidt et al. 2008). It is the first satellite remote sensing mission that can observe temporal variations of Earth's gravitational potential and examined long-term variation of terrestrial water storage (TWS) under all types of terrestrial conditions on the earth's surface (Rodell et al. 2004). This data provides variances of vertically integrated TWS, which is the sum of all surface water, soil moisture, snow, and ground water availability. The TWS generally includes all phases of water storage above (e.g., reservoirs and lakes) and below the surface of the Earth (Hassan and Jin 2014). The GRACE product is provided by three processing centers, including Geoforschungs Zentrum Potsdam (GFZ), the Jet Propulsion Laboratory (JPL), and the Center for Space Research (CSR) at the University of Texas (Jin et al. 2012). These datasets have been used in several studies around the world, including India (Rodell et al. 2008), East Africa (Becker et al. 2010), Turkey (Lenk 2013), China (Cao et al. 2015; Li et al. 2016), and South Korea (Lee et al. 2014; Seo and Lee 2016). Tapley et al. (2004) compared the variation in the geoid height from the GRACE and Global Land Data Assimilation System (GLDAS) over a global scale. Lee et al. (2014)

validated a terrestrial water storage model by comparing its estimates to the GLDAS and GRACE datasets on the Korean peninsula. Cao et al. (2015) also validated the terrestrial water storage change from GRACE as compared to that simulated from a hydrological model over northwest China from the year 2003–2012. Li et al. (2016) studied the water storage variation in the Yellow river basin using GRACE and other satellite datasets. Mo et al. (2016) compared the water storage variation measured from GRACE with the output of GLDAS in China. In this study, monthly GRACE mascons (i.e., mass concentration solutions) from the Center for Space Research (CSR RL05 mascons) (Save et al. 2016) dataset, which has a spatial resolution of $0.5° \times 0.5°$ was used. Save et al. (2016) and Scanlon et al. (2016) demonstrated that this dataset provided reducing leakage effect of land and ocean.

Water budget equation

Generally, the water balance shows seasonal patterns. In wet seasons, P is larger than ET, thereby creating a water surplus. However, in dry seasons, ET necessarily exceeds P (Zhang et al. 2008; Chen et al. 2013; Greve et al. 2016). Therefore, either the water surplus decreases or water deficits occur during dry seasons. The water budget is based on the principle of mass conservation, also known as the continuity equation. This can be defined through Eq. 1 as the balance between P, ET, and the change in water storage at the Earth's surface.

$$Q_N = P_N - ET_N - \Delta S_N \quad (1)$$

$$\Delta S_N = S_N - S_{N-1} \quad (2)$$

where ΔS is the change in water storage and N is the satellite- and ground-based measurement period. In this study, in order to estimate the water budget on a monthly timescale, the estimated ET and P are obtained from the COMS and GLDAS datasets. The TWS estimated from GRACE is a combined contribution of soil moisture in all layers, accumulated snow, plant canopy surface water and ground water (Zhou et al. 2016). Thus, in order to estimate the change in water storage on water budget equation (Eq. 1), we used the central difference method (Riegger and Tourian 2014) that was the difference of month to month variations of the TWS estimated from GRACE (Seo and Lee 2017). The summaries of satellite and model datasets used in this study for estimating the water budget are given in (Table 1).

Results and discussion

Intercomparison of GLDAS, and COMS with flux tower

Evapotranspiration

Figure 2 shows the temporal variation of ET from the flux tower, COMS, and GLDAS for both CFC and SMC sites. Figure 2 shows that GLDAS and COMS ET patterns varied depending on the vegetative growth conditions, and also showed a reasonable trend, with increasing ET coinciding with warm temperatures and high humidity in the summer monsoon season. The COMS and GLDAS datasets tend to show a slight underestimation of ET at the CFC site better than that of SMC site. Similar results and discrepancies were also found by Baik and Choi (2015a, b). In particular, as shown in Fig. 2, the GLDAS ET showed underestimation compared to flux tower measurement. The tendency for GLADS to underestimate ET is supported by Kalma et al. (2008), who demonstrated that uncertainty of GLDAS ET product results in errors greater than 25%. Smith et al. (2001) reported that this discrepancy may be caused by uncertainties of GLDAS datasets, which inherently result from the process of assimilating forcing data. Additionally, Baik and Choi (2015b) attributed the errors in ET estimates to incorrect information resulting from scale mismatches between different datasets. The statistical results of ET estimation for each dataset are presented in Table 2. The comparison between COMS ET and flux tower ET showed that the bias, root-mean-square rrror (RMSE), and correlation coefficient (R) were − 2.50, 39.64 mm/month, and 0.84 at CFC and 17.54, 23.73 mm/month, and 0.93 at SMC, respectively. The comparison between GLDAS and the flux tower ET showed that the bias, RMSE, and R were − 31.73, 45.17 mm/month, and 0.89 at CFC, − 15.51, 15.02 mm/month, and 0.97 at SMC, respectively (Table 2).

Precipitation

For analyzing the precipitation results, two flux tower sites were selected for validation before estimating the water budget equation using COMS RI, COMS CM, and GLDAS, and the two flux tower sites. A monthly time series of the precipitation measured at each of the two flux tower sites, from the months of April to December, 2011, is shown in Fig. 3, and the statistical results of the precipitation from each dataset are summarized in Table 2. As shown in Fig. 3, the precipitation of COMS RI showed under- and overestimation patterns, although

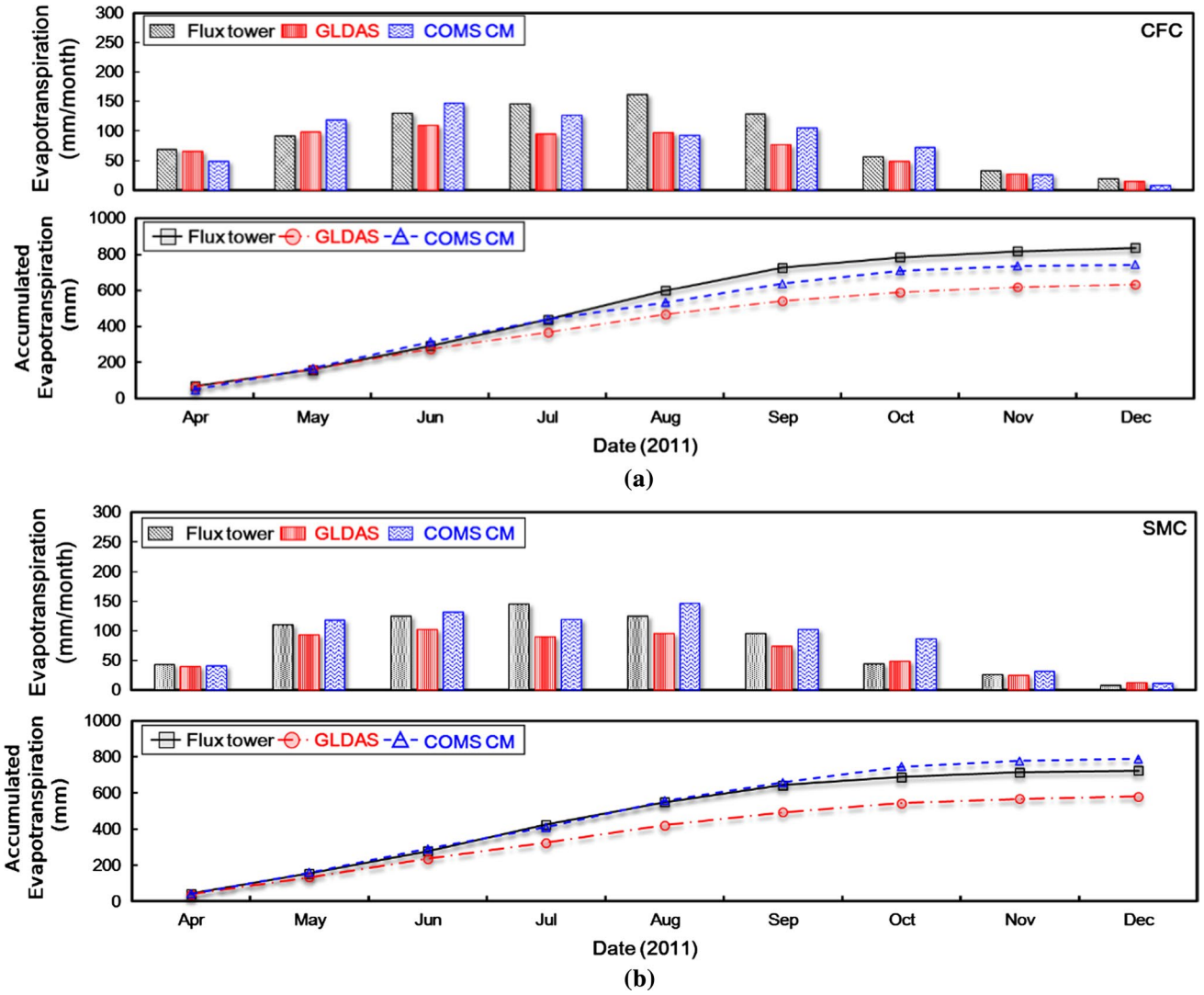

Fig. 2 Monthly and accumulated evapotranspiration estimated from model- and satellite-based dataset and measured from flux tower at CFC and SMC sites

that of each dataset showed reasonable agreement when compared to the flux tower. Similar results were also found in previous studies. Baik and Choi (2015c) reported that the COMS RI is computed using the relationship between cloud brightness temperature and SSM/I rainfall data. For this reason, the discrepancy between COMS RI and ground-based measurement was attributed to the differences in measurement techniques (i.e., the infrared rainfall retrieval algorithm) of COMS. As expected, the time series of accumulated precipitation from COMS CM showed an improvement when it was compared with COMS RI at the two flux tower sites (Fig. 3). The statistical results of the COMS CM (R of 0.99 and 0.99 at CFC and SMC, respectively) showed better performances than that of the COMS RI (R of 0.91 and 0.92 at the CFC and SMC, respectively). Also, the COMS CM (bias of − 7.99 and 30.93 mm/month, and RMSE of 49.98 and 43.04 mm/month at CFC and SMC sites, respectively) showed improvement by reducing bias and RMSE compared to the COMS RI (bias of − 82.20 and − 42.38 mm/month, and RMSE of 161.87 and 147.49 mm/month at the CFC and SMC sites, respectively). As shown in Table 2, the monthly and accumulated precipitation estimated from GLDAS showed reasonable agreement with that of the flux towers, though precipitation was underestimated at both flux towers (bias of − 22.22 and − 23.36 mm/month, and RMSE of 78.40 and 103.67 mm/month at CFC and SMC sites, respectively) due to differences in the forcing datasets.

Table 2 Comparison between hydrological variables estimated from each datasets

Dataset	Site	COMS ET	GLDAS
Evapotranspiration (ET)			
	CFC		
	Bias	− 2.50	− 31.73
	RMSE	39.64	45.17
	R	0.84	0.89
	SMC		
	Bias	17.54	− 15.51
	RMSE	23.73	15.02
	R	0.93	0.97

Dataset	Site	COMS RI	COMS CM	GLDAS
Precipitation (P)				
	CFC			
	Bias	− 82.20	− 7.99	− 22.22
	RMSE	161.87	49.98	78.40
	R	0.91	0.99	0.96
	SMC			
	Bias	− 42.38	30.93	− 23.36
	RMSE	147.49	43.04	103.67
	R	0.92	0.99	0.96

Runoff (R)	Site	COMS RI	COMS CM	GLDAS
	CFC			
	Bias	− 71.96	2.26	0.46
	RMSE	149.69	42.53	62.28
	R	0.66	0.99	0.96
	SMC			
	Bias	− 49.70	23.60	− 7.63
	RMSE	140.82	43.24	89.93
	R	0.74	0.99	0.96

The Bias and RMSE have units mm/month

Runoff

Figure 4 shows the variation of change in water storage estimated from GRACE TWS. As expected, this figure indicates that the seasonal cycles of the change in water storage results in a variation of between − 40 and 50 mm/month with a positive change mostly in the summer season and a negative change in the winter and spring seasons. Similar variation of the change in water storage was reported in the previous study (Seo and Lee 2017). Seo and Lee (2017) indicated that the change in water storage on the summer season showed a distinct pattern in relation to the heavy precipitation. If the precipitation increases in the summer season, more water resources can be stored in an area (Haile 2011). Thus, it can be inferred that an increase in the change in water storage estimated from GRACE can be associated with an increase in the amount of P or a decrease in ET (Li et al. 2016). A comparison of runoff estimated from ground data and another dataset using the change in water storage estimated from GRACE showed reasonable agreement (Fig. 4). As expected, the runoff estimated from COMS CM showed improved correlation, bias, and RMSE compared to that of the original COMS RI (Table 2; Fig. 4). In the CFC site, the results of monthly and accumulated runoff showed a reasonable correspondence among in situ, GLDAS, and COMS CM (Fig. 4) measurements. However, in the SMC site, accumulated runoff results of COMS CM and GLDAS indicated a slight tendency toward over- and underestimation compared to that of in situ measurements due to the mountainous topographical characteristics of the SMC site.

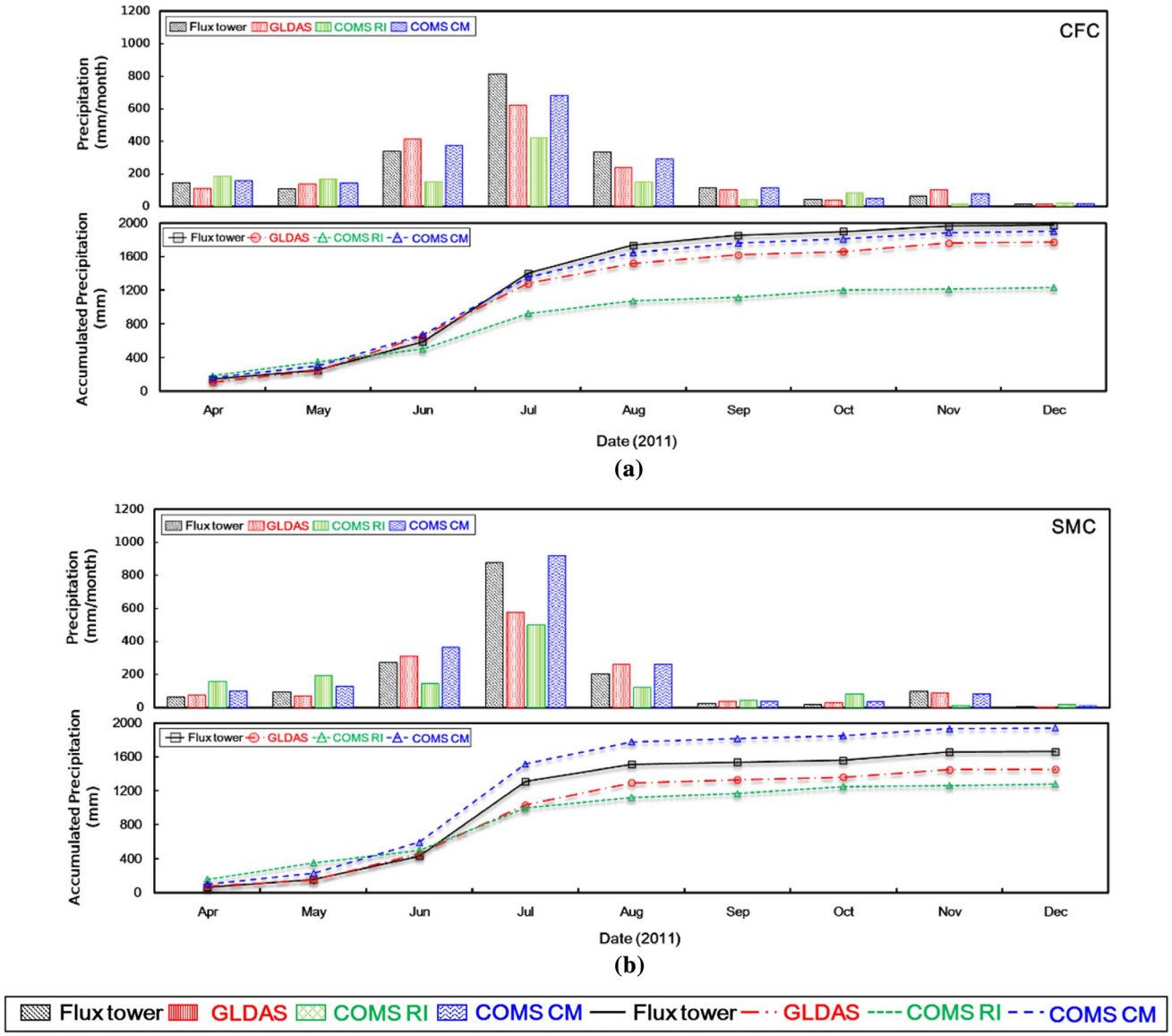

Fig. 3 Monthly and accumulated precipitation estimated from model- and satellite-based datasets and obtained from flux tower dataset at CFC and SMC sites

Spatial comparison of hydrological variables from GLDAS and COMS

Precipitation

Figures 5 and 6 show the spatial distribution of monthly precipitation and correlation maps of precipitation reported by each dataset over the study period. The spatial distribution of the ASOS is produced from 93 meteorological station datasets collected from the KMA. Overall, the accumulated precipitation ranged from 100 to 1100 mm, showing an increase from May to August and a decrease from September to November. Figure 5 shows that there is a slightly difference in spatial distributions between ASOS and COMS RI datasets over the entire territory of South Korea. The COMS RI displayed an overestimation pattern in pre-monsoon periods and showed underestimation during monsoon seasons. Similar uncertainties were also found in Baik et al. (2016) and Tuttle et al. (2008). Baik et al. (2016) reported that these uncertainties of COMS RI arose from its indirect rainfall estimation algorithm (i.e., infrared rain-retrieval method) that relies on the cloud-top brightness temperature in the infrared or visible bands (Scofield and Kuligowski, 2003; Tuttle et al. 2008). For this reason, COMS RI may be missing heavy and light precipitation in mountainous areas and may not capture rapid convective rainfall, hence resulting in under- and overestimation patterns (Baik and Choi 2015c). To

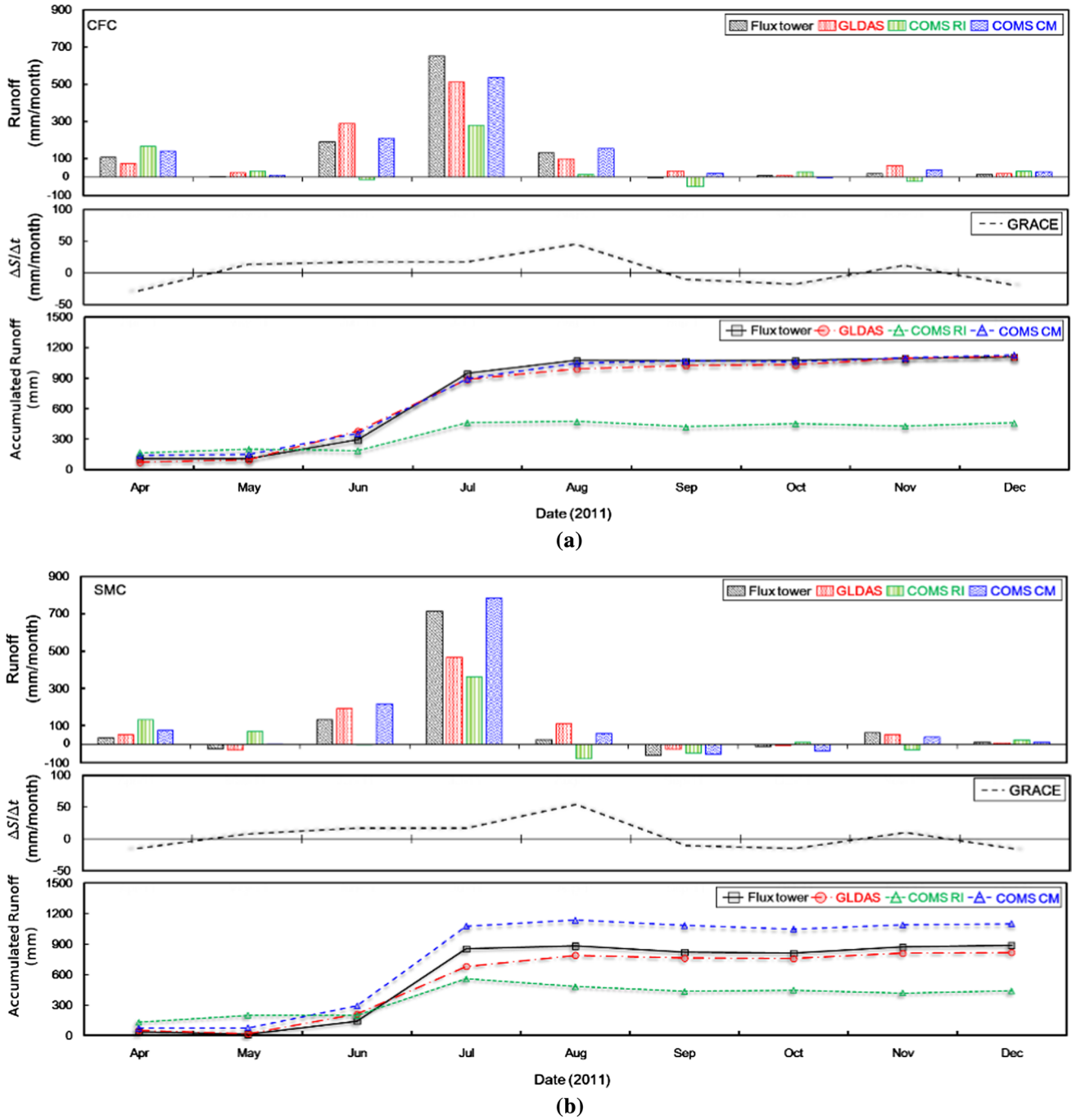

Fig. 4 Monthly and accumulated runoff estimated from model- and satellite-based datasets and obtained from flux tower dataset at CFC and SMC sites

reduce this uncertainty, the use of COMS CM applying the CM method showed good agreement with the spatial distribution of ASOS. These results were influenced by adopting the advantages of both ground-based and spatially distributed COMS RI data (Baik et al. 2016). As expected, the results of COMS CM presented in this study indicate that the use of the CM method has the potential to improve the COMS RI datasets. Moreover, as shown in Fig. 6, the COMS CM data showed a close similarity with the distribution of ASOS, with a level of agreement that rivaled that of other datasets. The spatial distribution of GLDAS, which combines a reanalyzed dataset using information such as ground-based and remote sensing observations (Rodell et al. 2004; Wang and Zeng 2012),

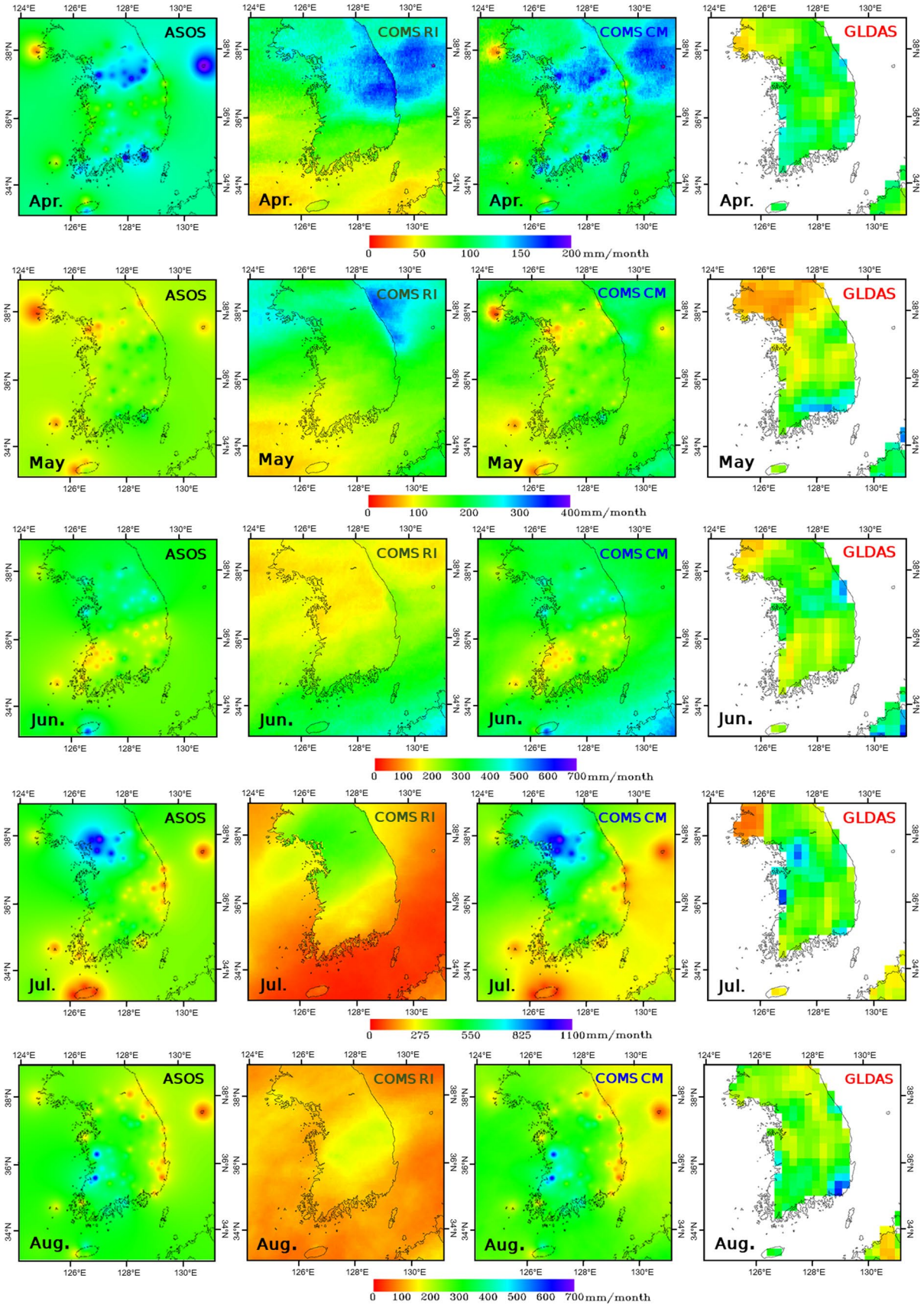

Fig. 5 Maps of precipitation from Interpolated ASOS, COMS RI, COMS CM, and GLDAS

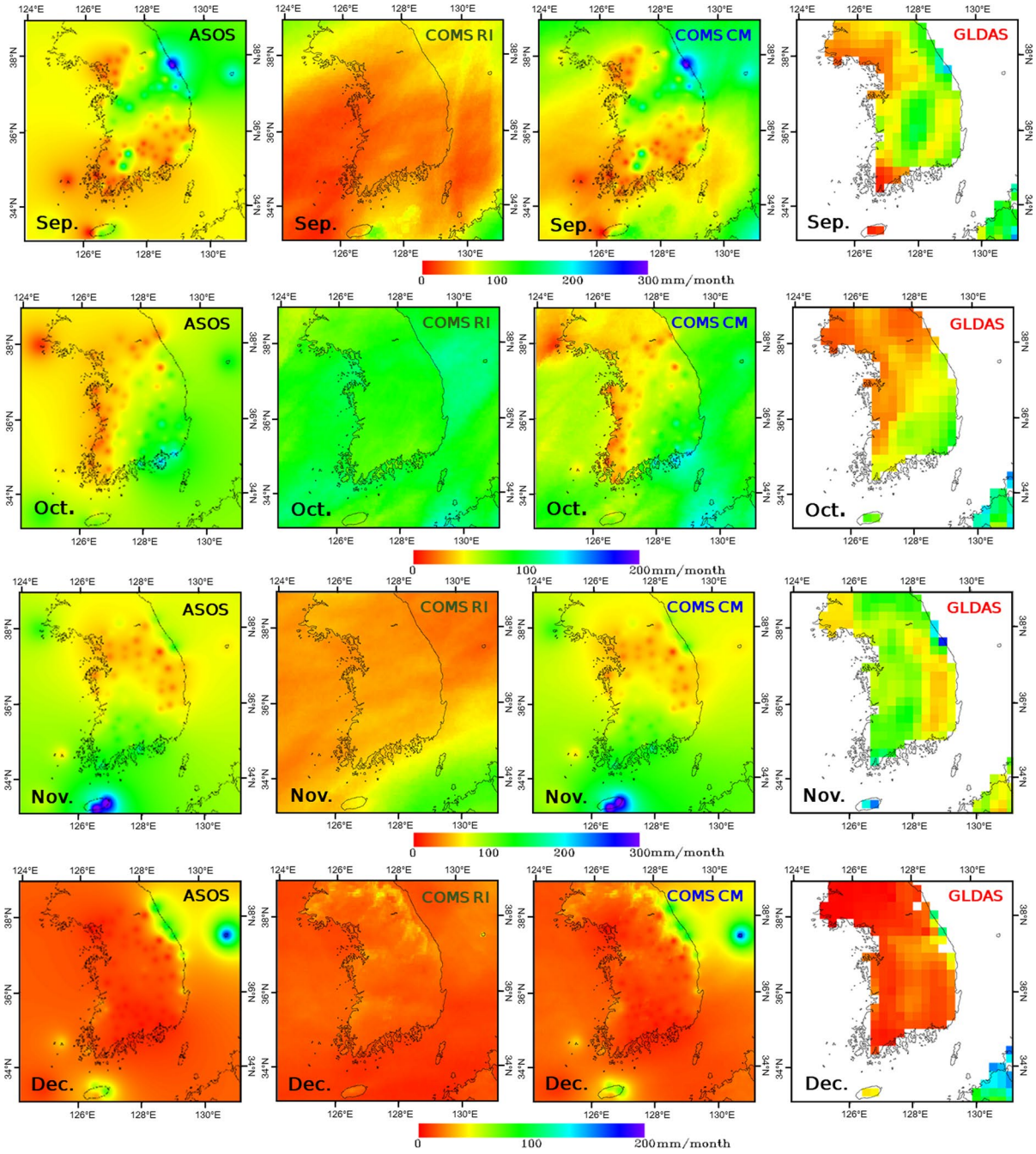

Fig. 5 (continued)

showed similar patterns compared with that of ASOS and COMS CM. However, GLDAS show different patterns in coastal and mountain areas relative to the ASOS data. Furthermore, the precipitation GLDAS dataset showed a low correlation with the distribution map of ground-based precipitation, except in flat areas. The reason for this discrepancy may be the coarse resolution of GLDAS data, which makes it difficult to record the spatial–temporal variability of precipitation within its pixels. Kalma et al. (2008) and Rodell et al. (2004) noted that precipitation dataset is among the most uncertain GLDAS datasets, with an uncertainty greater than 10%. Overall, the correlation analysis of COMS CM and GLDAS showed strong positive relationships when compared to the correlations of COMS RI. Based on these results, precipitation estimates from COMS CM and GLDAS provide results superior

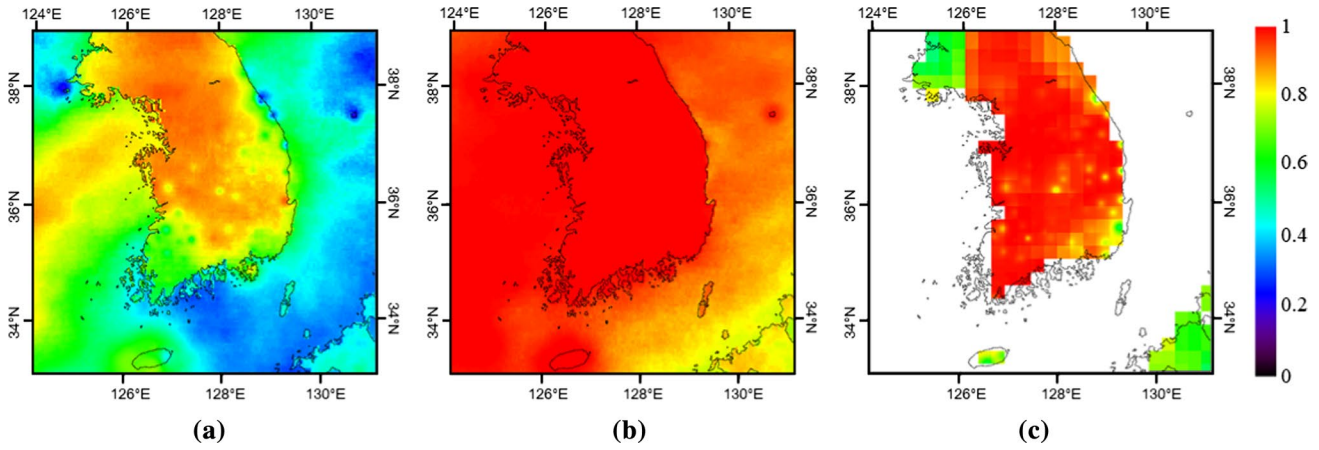

Fig. 6 Spatial patterns of correlation precipitation map for COMS RI, COMS CM, and GLDAS. **a** ASOS versus COMS RI, **b** ASOS versus COMS CM, **c** ASOS versus GLDAS

to those for COMS RI in terms of the water budget over South Korea.

Evapotranspiration

Figure 7 shows the spatial distribution of monthly ET from COMS and GLDAS over the study period. The ranges of ET estimated from COMS and GLDAS in each season are: spring (0–50 mm/month), summer (50–250 mm/month), autumn (20–150 mm/month), and winter (0–50 mm/month). As shown in Fig. 7, ET estimated from COMS captured all the pixels with more detail compared with the resolution of GLDAS. The spatial distribution of the COMS and GDLAS data showed slightly similar patterns (e.g., reached a maximum value in summer and decreased again in autumn) over South Korea. In other words, the onset of a temperature increase in the spring season initiates increases in the runoff and evaporative losses and hence decreases water storage, and the temperature and ET decrease at the end of the summer season. Nevertheless, the spatial distribution of the GLDAS data exhibited a lack of ability to observe ET near coastal regions due to its coarse resolution, whereas COMS can capture the ET in coastal areas due to its high spatial resolution. In the summer season, the spatial distribution of two datasets (i.e., COMS and GLDAS) displayed slightly different and distinct rainfall patterns. Figure 8 shows the average ET and the correlation maps of ET from the COMS and GLDAS satellites. Although the average patterns of COMS and GLDAS showed similar overall tendencies, the spatial distribution of the correlation between the COMS and GLDAS showed slight differences. This difference was attributed to the scale mismatch between COMS (1 km) and GLDAS (25 km) (Baik and Choi 2015b).

Runoff

Figure 9 shows the runoff as measured by COMS and GLDAS and the change in water storage of GRACE over the study period. Monthly runoff from both datasets ranged from − 100 to 1200 mm/month [e.g., spring (− 100 to 200 mm/month), summer (− 100 to 1200 mm/month), autumn (− 100 to 200 mm/month), and winter (− 100 to 100 mm/month)]. The runoff begins to rise gradually in May and increases rapidly with the start of the monsoon season. This change indicates that the increasing and decreasing trends of runoff are related to the patterns of precipitation and evapotranspiration (Li et al. 2016). As shown in Fig. 9, the runoff estimated from both datasets showed a reasonable agreement, although they showed different patterns in coastal and mountain areas. The correlation map of runoff between COMS and GLDAS in Fig. 10b also indicates a relatively better performance except for the mountainous territory in the East of South Korea and coastal areas on the three sides of the dataset. According to the above-mentioned results of precipitation and evapotranspiration, discrepancies in the results of GLDAS can be attributed to the impact on complex mountainous terrain (i.e., heterogeneous topography) and coastal areas that are poorly mapped due to the low spatial resolution of 25 km. As expected, the annual rainfall decreases in southern areas. The average map of the runoff estimated from COMS and GLDAS (Fig. 10a) and the annual precipitation provided by the annual climatological report of the KMA over South Korea (Fig. 10c) displayed similar patterns because the amount of runoff is directly affected by the precipitation. The spatiotemporal comparison of COMS and GLDAS over the study period showed very similar patterns. However, the slight discrepancy between COMS and GLDAS is attributed to the spatiotemporal

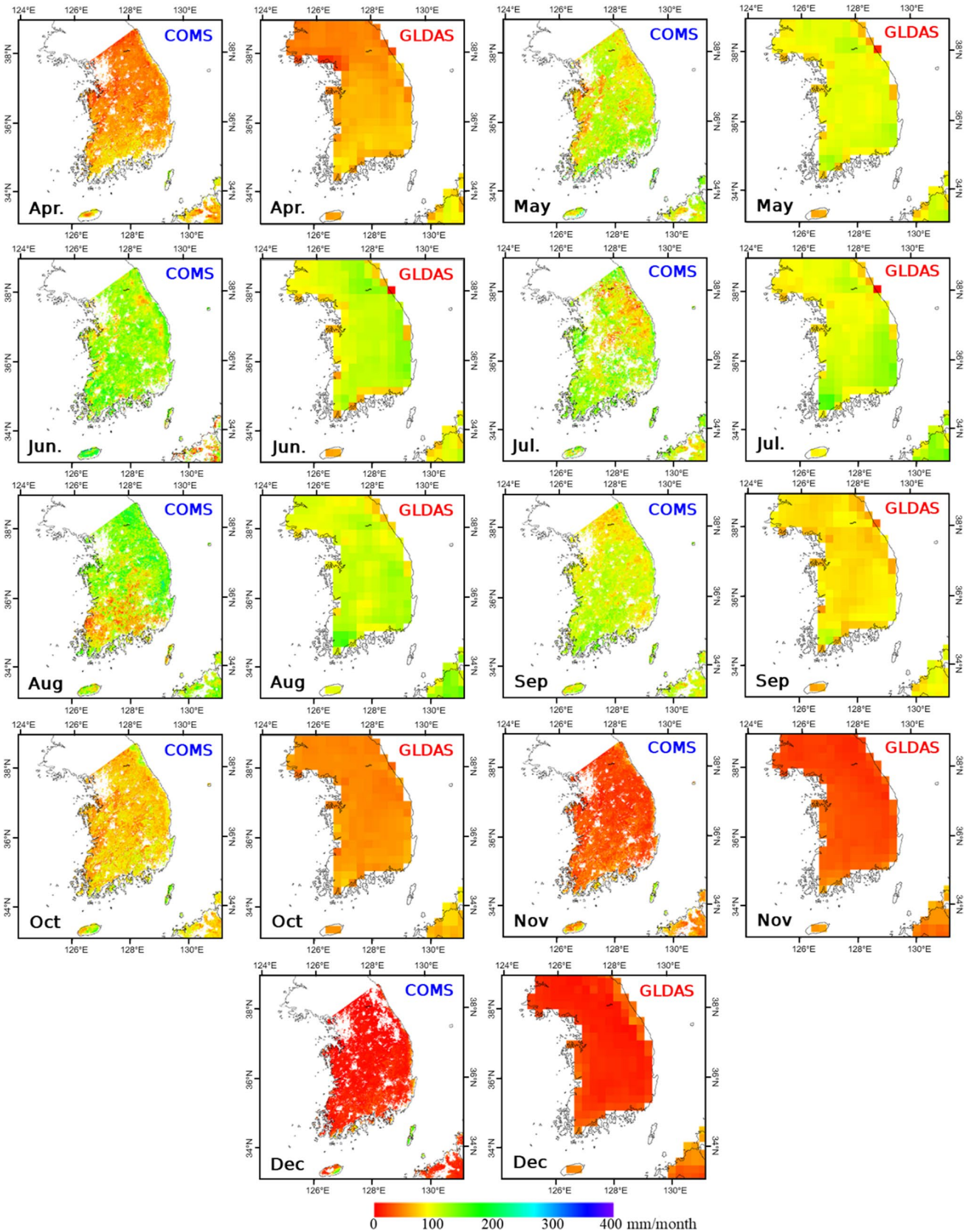

Fig. 7 Spatial distribution of the monthly evapotranspiration estimated from COMS dataset using the revised RS-PM model and provided from GLDAS dataset over the study periods (April 1–December, 2011)

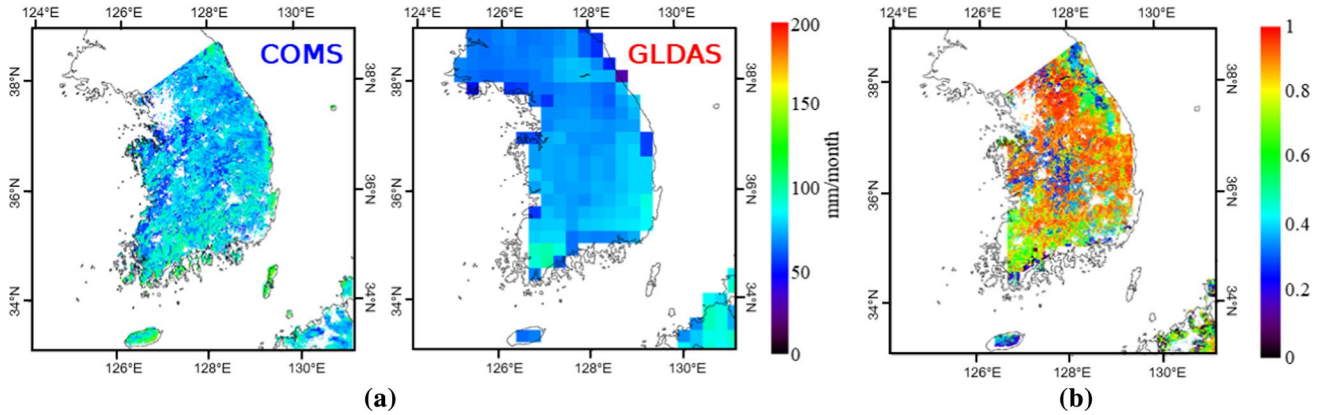

Fig. 8 Spatial patterns of average and correlation evapotranspiration maps for COMS and GLDAS over South Korea: **a** average map of COMS (left side) and GLDAS (right side) and **b** correlation map (GLDAS vs. COMS)

scale mismatch and the differences in measurement techniques (Baik and Choi 2015a).

Conclusion

The main objective of this study was to estimate the water budget from satellite-based datasets over South Korea. In order to apply the water budget equation, this study considered the P, ET, ΔS, and R quantities estimated and calculated from multiple remote sensing and model datasets (COMS, GLDAS, and GRACE). First, the ET is estimated from the revised RS-PM model using datasets from geostationary (COMS) satellites and from GLDAS. Theses ET estimates were evaluated at two flux tower sites (CFC and SMC) in South Korea. The statistical results of GLDAS and COMS ETs showed a reasonable agreement at the two flux towers. The spatial mapping of the COMS and GDLAS showed slightly similar patterns (e.g., reached a maximum value of ET in summer and decreased again in spring). Second, before considering the water budget equations over South Korea, this study compared precipitation estimated from GLDAS, COMS RI, and COMS CM, which uses the conditional merging method to improve the accuracy of the COMS RI quality, and evaluated these estimates at the two flux tower sites. The statistical results of COMS CM showed substantial improvements over COMS RI, as measured using the flux tower rainfall at the two flux tower sites. The spatial distribution of COMS CM and GLDAS data exhibited spatial patterns similar to the ASOS data, and again showed better agreement than the COMS RI dataset. Finally, this paper evaluated the water budget for South Korea from the various hydrological factors (i.e., P, ET, and R) estimated from the satellite products. The results showed that the runoff estimated from COMS CM improved the correlation, bias, and RMSE when compared to the runoff estimated from the original COMS RI. The correlation coefficients of COMS CM and GLDAS showed comparable agreements with the flux towers (0.99 and 0.96 at CFC, respectively, and 0.99 and 0.96 at SMC, respectively). The spatial patterns of runoff showed that the runoff distributions also behave similarly across models due to the influence of the rainfall distribution. However, the low spatial resolution of GLDAS means that it does a poor job of estimating meteorological variables in complex mountainous terrain (i.e., heterogeneous topography) in the Eastern region of South Korea. The spatial distribution of runoff estimated from COMS CM and GLDAS showed a reasonable performance. However, the slight difference between the COMS CM and GLDAS can be attributed to the spatial and temporal scale mismatch in the process of integrating the each dataset and differences in the algorithms for estimating the hydrological variables. Overall, the performance of COMS CM was comparatively superior due to its high spatial and temporal resolutions.

Possible causes of water shortages include increases in water usage, lack of available water resources in periods of drought, and the unequally distributed water resources under geographically biased rainfall patterns. Therefore, an accurate and consistent estimation of various hydrological variables is essential for understanding integrated water resource management, and for developing efficient water resource planning and monitoring projects. Further research and quantitative analysis is needed to realize the uses and dynamics of water resources, and to analyze and

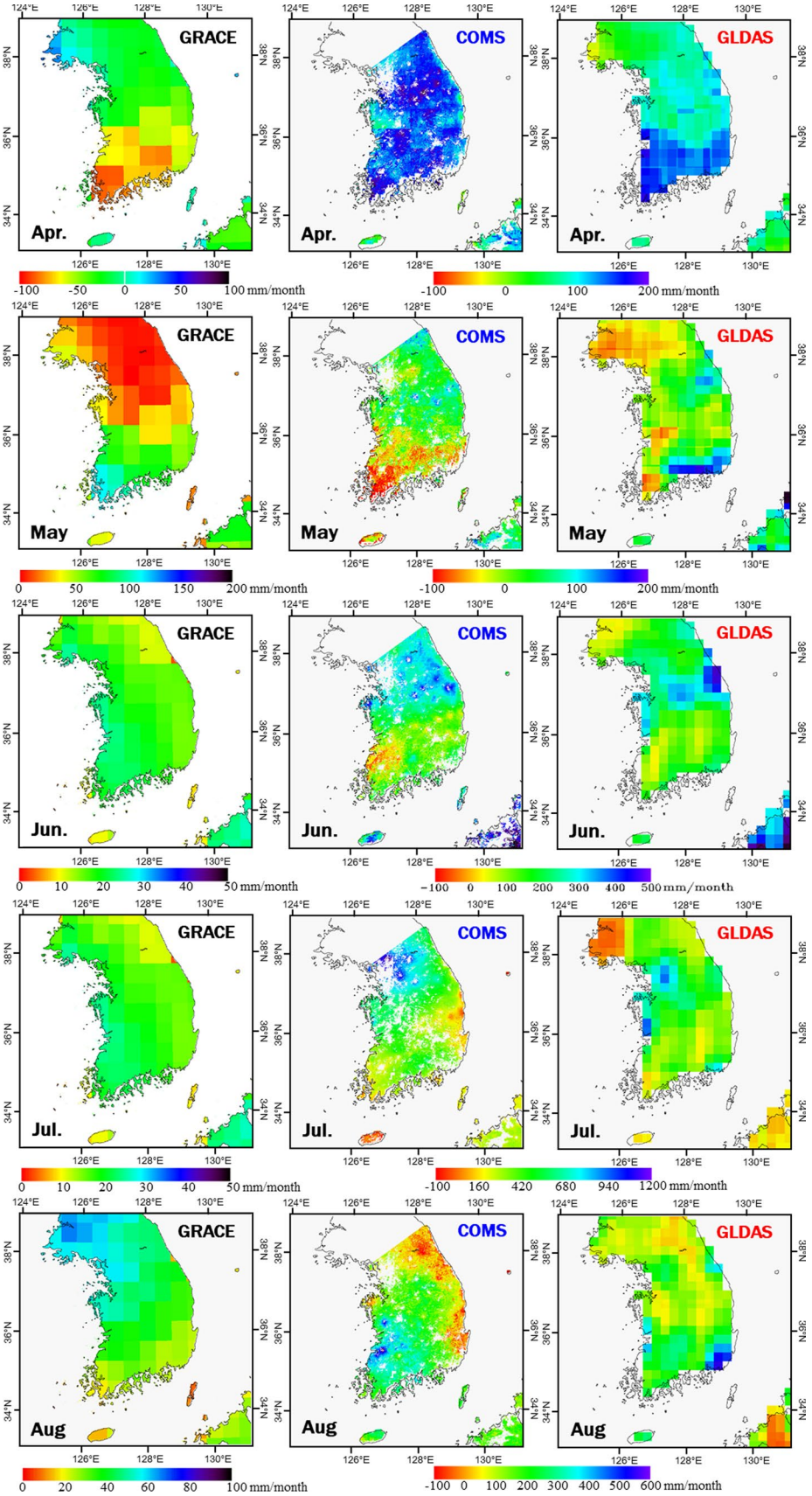

Fig. 9 Monthly runoff estimated from COMS (1 km) and GLDAS (25 km) dataset and monthly change in water storage estimated from GRACE (100 km) dataset in South Korea during April to December, 2011

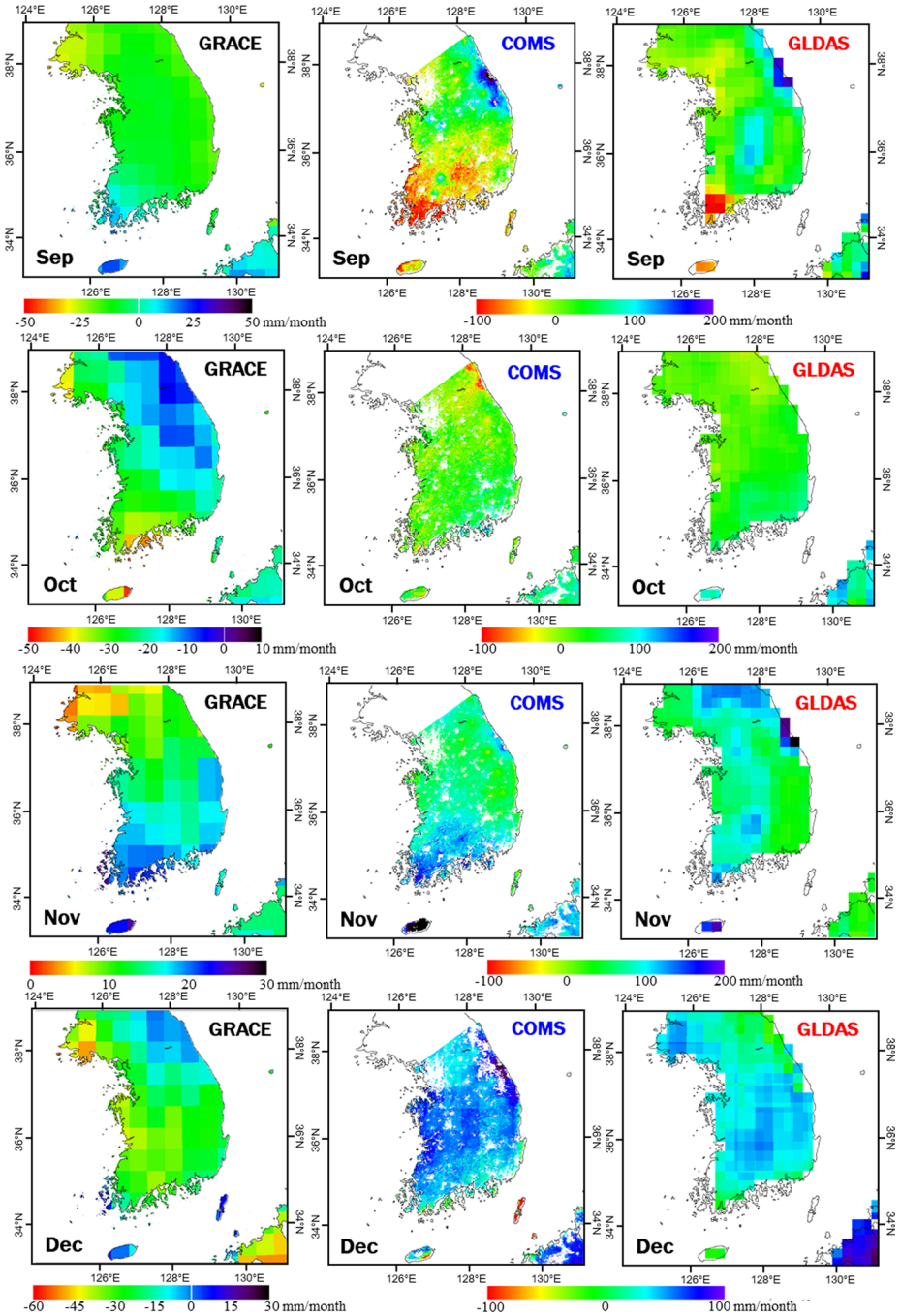

Fig. 9 (continued)

understand the spatio-temporal variability of P, ET, and R. The advantage of the COMS geostationary satellite is that it can be more widely applied across microclimates for analyzing complex hydrological phenomena, allowing for more efficient water resource planning and monitoring, and drought monitoring. The conditionally merged data from

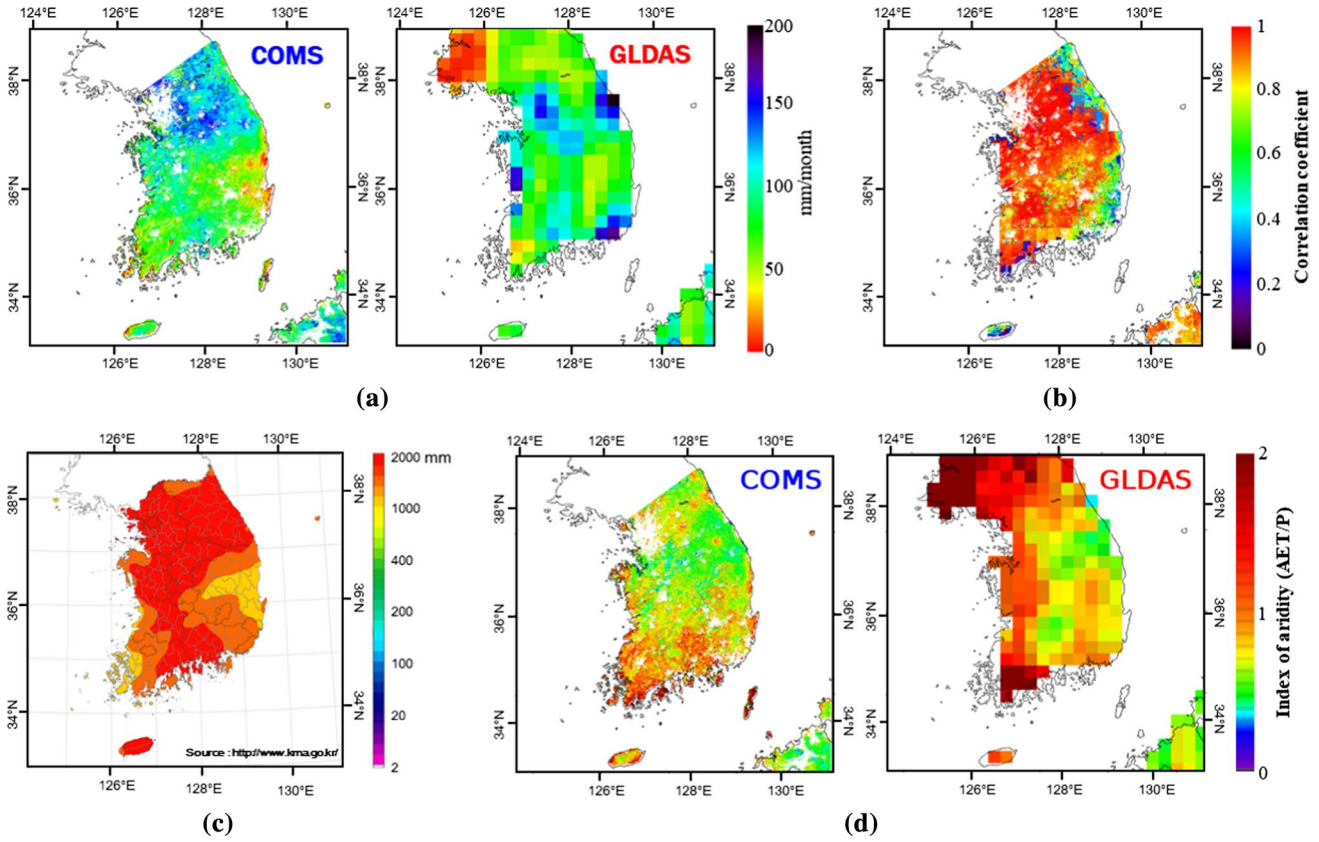

Fig. 10 Spatial patterns of runoff for **a** average maps from COMS and GLDAS, **b** correlation map (GLDAS vs. COMS); **c** annual precipitation map provided from KMA; **d** average evaporative index (AET/P) estimated from COMS and GLDAS

COMS are highly useful for obtaining valuable information at all-time steps and are available for analyzing hydrological phenomenon across Korea.

Acknowledgements This research was supported by a grant (17AWMP-B079625-04) from Water Management Research Program funded by Ministry of Land, Infrastructure and Transport of Korean government. This work was supported by the National Research Foundation of Korea (NRF) grant funded by the Korea government (MSIT) (NRF-2016R1A2B4008312). This research was supported by Space Core Technology Development Program through the National Research Foundation of Korea (NRF) funded by the Ministry of Science and ICT (NRF-2014M1A3A3A02034789).

References

An M-H (2007) Development of meterological data processing system of communication, ocean and meteorological satellite, Meteorological Research Institute, Republic of Korea

Baik J, Choi M (2015a) Evaluation of remotely sensed actual evapotranspiration products from COMS and MODIS at two different flux tower sites in Korea. Int J Remote Sens 36(1):375–402

Baik J, Choi M (2015b) Evaluation of geostationary satellite (COMS) based Priestley–Taylor evapotranspiration. Agric Water Manag 159:77–91

Baik J, Choi M (2015c) Spatio-temporal variability of remotely sensed precipitation data from COMS and TRMM: Case study of Korean peninsula in East Asia. Adv Space Res 56:1125–1138

Baik J, Park J, Ryu D, Choi M (2016) Geospatial blending to improve spatial mapping of precipitation with high spatial resolution by merging satellite- and ground based data. Hydrol Process 30(16):2789–2803. https://doi.org/10.1002/hyp.10786

Becker M, LLovel W, Cazenave A, Güntner A, Crétaux J-F (2010) Recent hydrological behavior of the East African great lakes region inferred from GRACE, satellite altimetry and rainfall observations. CR Geosci 342(3):223–233

Cao Y, Nan Z, Cheng G (2015) GRACE gravity satellite observations of terrestrial water storage changes for drought characterization in the arid land of northwestern China. Remote Sens 7(1):1021–1047

Chen X, Alimohammadi N, Wang D (2013) Modeling interannual variability of seasonal evaporation and storage change based on the extended Budyko framework. Water Resour Res 49:6067–6078

Greve P, Gudmundsson L, Orlowsky B, Seneviratne SI (2016) A two-parameter Budyko function to represent conditions under which evapotranspiration exceeds precipitation. Hydrol Earth Syst Sci 20:2195–2205. https://doi.org/10.5194/hess-20-2195-2016

Haile KH (2011) Estimation of terrestrial water storage in the upper reach of Yellow River. Diss. Master's thesis, retrieved from faculty

of geo-information science and earth observation library, University of Twente, Enschede, The Netherlands
Hassan AA, Jin S (2014) Lake level change and total water discharge in the East Africa Rift Valley from satellite-based observations. Global Planet Change 117:79–90
Jin SG, Hassan AA, Feng GP (2012) Assessment of terrestrial water contributions to polar motion from GRACE and hydrological models. J Geodyn 62:40–48. https://doi.org/10.1016/j.jog.2012.01.009
Kalma JD, McVicar TR, McCabe MF (2008) Estimating land surface evaporation: a review of methods using remotely sensed surface temperature data. Surv Geophys 29(4–5):421–469
Kang S, Doh S, Lee D, Lee D, Jin VL, Kimball JS (2003) Topographic and climatic controls on soil respiration in six temperate mixed-hardwood forest slopes, Korea. Glob Change Biol 9:1427–1437
Lee SI, Seo JY, Lee SK (2014) Validation of terrestrial water storage change estimates using hydrological simulation. J Water Resour Ocean Sci 3(1):5–9
Lenk O (2013) Satellite based estimates of terrestrial water storage variations in Turkey. J Geodyn 67:106–110
Li Q, Zhong B, Luo Z, Yao C (2016) GRACE-based estimates of water discharge over the Yellow River basin. Geod Geodyn 7(3):187–193
Marshall M, Tu K, Funk C, Michaelsen J, Williams P, Williams C, Ardö J, Boucher M, Cappelaere B, de Grandcourt A, Nickless A, Nouvellon Y, Scholes R, Kutsch W (2013) Improving operational land surface model canopy evapotranspiration in Africa using a direct remote sensing approach. Hydrol Earth Syst Sci 17:1079–1091. https://doi.org/10.5194/hess-17-1079-2013
Miralles DG, Holmes TRH, De Jeu RAM, Gash JH, Meesters AGCA, Dolman AJ (2011) Global land-surface evaporation estimated from satellite-based observations. Hydrol Earth Syst Sci 15:453–469
Mitsch WJ, Gosselink JG (2000) The value of wetlands: importance of scale and landscape setting. Ecol Econ 35(1):25–33
Mo X, Wu JJ, Wang Q, Zhou H (2016) Variations in water storage in China over recent decades from GRACE observations and GLDAS. Nat Hazards Earth Syst Sci 16:469–482
Mu Q, Heinsch FA, Zhao M, Running SW (2007) Development of a global evapotranspiration algorithm based on MODIS and global meteorology data. Remote Sens Environ 111(4):519–536. https://doi.org/10.1016/j.rse.2007.04.015
Munier S, Aires F, Schlaffer S, Prigent C, Papa F, Maisongrande P, Pan M (2014) Combining data sets of satellite-retrieved products for basin-scale water balance study: 2. Evaluation on the Mississippi Basin and closure correction model. J Geophys Res Atmos 119, 12, 100–12, 116, https://doi.org/10.1002/2014jd021953
Nam W-H, Hong E-M, Choi J-Y (2015) Has climate change already affected the spatial distribution and temporal trends of reference evapotranspiration in South Korea? Agric Water Manag 150:129–138
Oki Taikan, Kanae S (2006) Global hydrological cycles and world water resources. Science 313(5790):1068–1072. https://doi.org/10.1126/science.1128845
Oliveira PTS, Nearing MA, Moran MS, Goodrich DC, Wendland E, Gupta HV (2014) Trends in water balance components across the Brazilian Cerrado. Water Resour Res 50:7100–7114
Park SK, Lee E (2007) Synoptic features of orographically enhanced heavy rainfall on the east coast of Korea associated with Typhoon Rusa (2002). Geophys Res Lett 34:L02803
Park S, Lee Y, Lee BS, Hwang Y, Lee U (2011) Implementation and validation of earth acquisition algorithm for communication, ocean and meteorological satellite. J Astron Space Sci 28:345–354
Park J, Baik J, Choi M (2017) Satellite-based crop coefficient and evapotranspiration using surface soil moisture and vegetation indices in Northeast Asia. CATENA 156:305–314
Ramillien G, Famiglietti JS, Wahr J (2008) Detection of continental hydrology and glaciology signals from GRACE: a review. Surv Geophys 29:361–374
Riegger J, Tourian MJ (2014) Characterization of runoff-storage relationships by satellite gravimetry and remote sensing. Water Resour Res 50:3444–3466
Rodell M, Houser PR, Jambor U, Gottschalck J, Mitchell M, Meng CJ, Arsenault K, Cosgrove B, Radakovich J, Bosilovich M, Entin JK, Walker JP, Lohmann D, Toll D (2004) The global land data assimilation system. BAMS. https://doi.org/10.1175/BAMS-85-3-381
Rodell M, Velicogna I, Famiglietti JS (2008) Satellite-based estimates of groundwater depletion in India. Nature 460:999–1002
Ryu J-H, Han H-J, Cho S, Park Y-J, Ahn Y-H (2012) Overview of geostationary ocean color imager (GOCI) and GOCI data processing system (GDPS). Ocean Sci J 47:223–233
Sahoo AK, Pan M, Troy TJ, Vinukollu RK, Sheffield J, Wood EF (2011) Reconciling the global terrestrial water budget using satellite remote sensing. Remote Sens Environ 115(8):1850–1865
Save H, Bettadpur S, Tapley BD (2016) High-resolution CSR GRACE RL05 mascons. J Geophys Res Solid Earth 121(10):7547–7569
Scanlon BR, Zhang Z, Save H, Wiese DN, Landerer FW, Long D, Longuevergne L, Chen J (2016) Global evaluation of new GRACE mascon products for hydrologic applications. Water Resour Res 52:9412–9429
Schmidt R, Flechtner F, Meyer U, Neumayer KH, Dahle C, Koenig R, Kusche J (2008) Hydrological signals observed by the GRACE satellites. Surv Geophys 29:319–334
Scofield RA, Kuligowski RJ (2003) Status and outlook of operational satellite precipitation algorithms for extreme-precipitation events. Weather Forecast 18(6):1037–1051
Seo JY, Lee SI (2016) Integration of GRACE, ground observation, and land-surface models for groundwater storage variations in South Korea. Int J Remote Sens 37(24):5786–5801
Seo JY, Lee SI (2017) Total discharge estimation in the Korean peninsula using multi-satellite products. Water 9(7):532–540. https://doi.org/10.3390/w9070532
Sheffield J, Ferguson CR, Troy TJ, Wood EF, McCabe MF (2009) Closing the terrestrial water budget from satellite remote sensing. Geophys Res Lett 36:L07403. https://doi.org/10.1029/2009GL037338
Sinclair S, Pegram G (2005) Combining radar and rain gauge rainfall estimates using conditional merging. Atmos Sci Lett 6(1):19–22
Smith SR, Legler DM, Verzone KV (2001) Quantifying uncertainties in NCEP reanalysis using high-quality research vessel observations. J Clim 14:4062–4072
Tapley BD, Bettadpur S, Ries JC, Thompson PF, Watkins MM (2004) GRACE measurements of mass variability in the Earth system. Science 305(5683):503–505
Thiemig V, Rojas R, Zambrano-Bigiarini M, Levizzani V, De Roo A (2012) Validation of satellite-based precipitation products over sparsely gauged African river basins. J Hydrometeorol 13(6):1760–1783
Thomas V, Albert JRG, Hepburn C (2014) Contributors to the frequency of intense climate disasters in Asia-Pacific countries. Clim Change 126(3–4):381–398. https://doi.org/10.1007/s10584-014-1232-y
Tuttle JD, Carbone RE, Arkin PA (2008) Comparison of ground-based radar and geosynchronous satellite climatologies of warm-season precipitation over the United States. J Appl Meteorol Climatol 47(12):3264–3270
Wang A, Zeng X (2012) Evaluation of multi reanalysis products with in situ observations over the Tibetan Plateau. J Geophys Res 117:D05102. https://doi.org/10.1029/2011JD016553
Wang H, Guan H, Gutiérrez-Jurado HA, Simmons CT (2014) Examination of water budget using satellite products over Australia. J Hydrol 511:546–554

Woldemeskel FM, Sivakumar B, Sharma A (2013) Merging gauge and satellite rainfall with specification of associated uncertainty across Australia. J Hydrol 499:167–176

Zhang L, Potter N, Hickel K, Zhang Y, Shao Q (2008) Water balance modeling over variable time scales based on the Budyko framework—model development and testing. J Hydrol 360:117–131

Zhou Y, Jin S, Tenzer R, Feng J (2016) Water stograge variations in the Poyang Lake Basin estimated GRACE and satellite altimetry. Geod Geodyn 7(2):108–116